# Survivable Hybrid Passive Optical Converged Network (HPCAN) Architectures Based on Reflective Monitoring

Elaine Wong[1], Carmen Mas Machuca[2], and Lena Wosinska[3]

[1]Department of Electrical and Electronic Engineering, The University of Melbourne, VIC 3010, Australia.
[2]Technical University of Munich (TUM), 80333 Munich, Germany.
[3]School of ICT., KTH Royal Institute of Technology, 16440 Kista, Sweden.

*Abstract—* **Hybrid Passive Optical Converged Access Networks (HPCANs) are recognised as a cost-efficient and high-bandwidth solution to address the exponentially increasing demands of both fixed access and mobile users. HPCANs are expected to support high client count with different bandwidth requirements, long network spans, and high traffic. In that respect, survivability of such networks against fiber/equipment failures is a critical deployment feature. Consequently, rapid fault detection and subsequent restoration of services to users are gaining importance. Four survivable architectures that are compliant with the aforementioned HPCAN specifications are presented in this work. These architectures do not need to rely on upstream transmissions for Loss-Of-Signal (LOS) activation, thereby making them suitable for use with sleep/doze mode transceivers for power-saving. In networks that implement sleep/doze upstream transceivers, the transition into sleep/doze mode would result in no upstream signal transmission. If using conventional LOS activation rather than our proposed architectures to indicate equipment/fiber failure in the network, the absence of upstream transmission would result in erroneous triggering of false LOS alarm and subsequently unnecessary protection switching. We compare the four survivable HPCAN architectures against an unprotected HPCAN using illustrative examples of three different population densities, namely covering dense urban, urban, and rural areas, and three different deployment scenarios, namely brownfield, duct reuse, and greenfield. We perform detailed evaluations of connection availability, failure-impact-factor, yearly network energy consumption, and total network cost. Results from this study provide guidance for the choice of the best survivable HPCAN architecture to serve each of the three considered area densities under each of the three deployment scenarios.**

*Index Terms—***Converged access network, hybrid time and wavelength division multiplexing, network protection and restoration, survivability.**

Elaine Wong (e-mail: ewon@unimelb.edu.au) is with the Department of Electrical and Electronic Engineering, The University of Melbourne, Melbourne, VIC 3010, Australia.
Carmen Mas Machuca is with the Technische Universität München (TUM) 80333 Munich, Germany.
Lena Wosinska is with the School of ICT., KTH Royal Institute of Technology, 16440 Kista, Sweden.

## I. INTRODUCTION

Major carriers have indicated that the following requirements need to be addressed when choosing the next access network technology solution, i.e. the Next Generation Passive Optical Networks 2 (NGPON2): (a) concurrent support of legacy, new, and mobile backhaul services; (b) reuse of existing Optical Distribution Network (ODN); (c) flexible bandwidth upgradeability and management; (d) support of high bandwidth/capacity and client count; (e) optimized technology combinations in terms of cost, performance and energy savings; and (f) *implementation of non-intrusive fault diagnostics with rapid restoration of services* [1-2]. In that respect, Hybrid Passive Optical Converged Access Networks (HPCANs) have been proposed to address the above requirements through supporting both fixed access as well as mobile backhaul [3]. HPCANs exploit the high bandwidth and flexibility features of Wavelength Division Multiplexing (WDM) whilst benefiting from cost-sharing and statistical multiplexing features of Time Division Multiplexing (TDM). Multi-rate transmission combining dedicated high bandwidth and time-shared wavelength channels can thus be deployed.

A comparison of a typical legacy TDM-PON and a HPCAN is shown in Fig. 1. Benefiting from the combination of WDM and TDM, HPCANs can serve an increased number of clients, accommodate high bandwidth applications, and an increased network span that consolidates metro and access networks. The Main Central Office (MCO) functions to aggregate/separate traffic between the core and access segments, thus providing node consolidation of the metropolitan and multiple access networks. In the HPCAN, bandwidth-dedicated business customers and mobile customers, through Mobile Base Stations (MBSs), are directly connected to Remote Node 1 (RN1) which demuliplexes/multiplexes downstream/upstream wavelengths. In turn, each MBS is connected to the optical network through an optical network unit (ONU), which is designated unique downstream and upstream wavelength channels. Additionally, residential users are connected to Remote Node 2 (RN2) which implements bandwidth sharing via a power splitter.

In a traditional optical telecommunications network, the survivability of the core and metro segments is important as

any node/link failure will affect a large number of users. The increased cost from implementing protection and restoration mechanisms through network redundancy and switching is justifiable as the cost is shared between a high number of users [4]. Similarly, the survivability of HPCANs is just as crucial, in particular when HPCANs are expected to (a) replace metro networks which are traditionally protected, and (b) support a plethora of high-bandwidth services to a wide range of customer profiles, including high-value mobile x-hauling and business customers which expect guaranteed network availability.
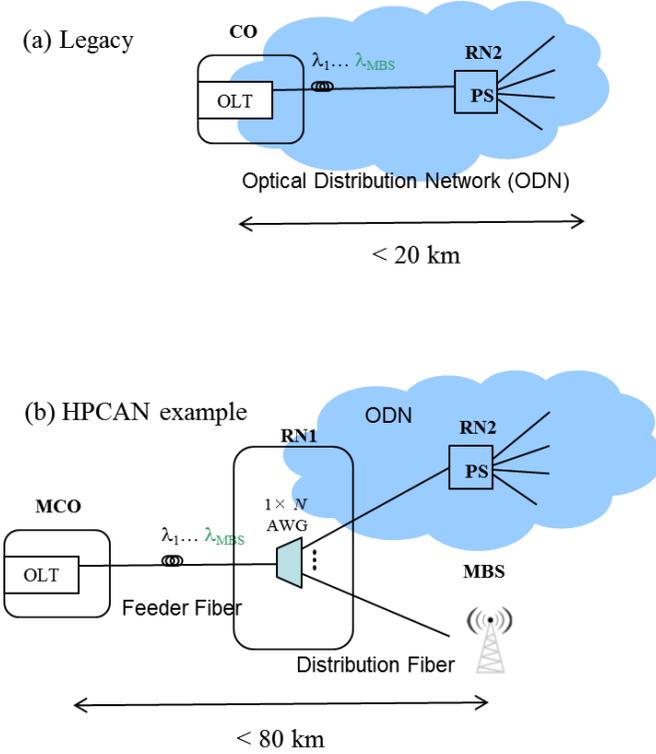


Fig. 1 Schematic of (a) legacy TDM-PON and (b) Hybrid Passive Converged Access Network (HPCAN). OLT is the Optical Line Terminal placed at the central Office (CO) or Main Central Office (MCO) when node consolidation is considered.

Protection of hybrid TDM/WDM PONs is a well-researched topic [5]-[8] where varying degrees of fiber/equipment duplication are implemented to achieve survivability. Nonetheless, currently proposed protection architectures, including those that are specified for HPCANs [9]-[10], assume the use of Loss-of-Signal (LOS) of upstream transmissions from ONUs to indicate equipment/fiber failure. Using LOS at the MCO may potentially be unsuitable in networks that implement sleep/doze mode operation. As the access segment was shown to be the dominant contributor to the overall power consumption of optical networks [11], power-saving operations have been introduced in access networks to reduce the power consumption of the ONUs [12]. During idle periods where no upstream data needs to be transmitted, sleep/doze capable transceivers of MBSs and ONUs can be powered down. If the LOS of upstream transmissions is used at the MCO to detect faults, erroneous triggering of false LOS alarm and subsequently erroneous protection switching will occur during these idle transmission periods when MBSs and/or ONUs are sleeping or dozing. Therefore, in such cases, the absence of upstream signals detected at the MCO *cannot* be considered as a true indication of LOS.

To address the reliability requirements of future energy-efficient networks where sleep/doze mode operation may be implemented, four power-saving survivable HPCAN architectures were introduced in [13] with the aim to *protect against high-impact failures on the working path that affect the MBS*. The proposed architectures were designed to accommodate sleep/doze mode capable transceivers, and do not require upstream transmissions from these transceivers to indicate LOS. Instead, the survivable architectures implement a continuous wave (CW) monitoring light that originates at the MCO and is launched into the optical distribution network (ODN) to be *optically looped back* for fault detection. Specifically, each of the survivable HPCAN architectures exploits highly-sensitive monitoring modules with fast-response fault detection and subsequent protection switching times [13]. In turn, each monitoring module comprises a monitoring transmitter (MON TX) and a monitoring receiver (MON RX). MON TX transmits and launches the monitoring signal, e.g. on channel $\lambda_M$, into the ODN. This signal is then optically looped back either at the remote node or at the input of each MBS and detected back at the OLT using MON RX. Previous experimental characterization of our purposefully built monitoring module showed that the looped back signal on $\lambda_M$ can be reliably detected by MON RX down to very low optical power levels of -51 dBm [14]. Such high receiver sensitivity allows the monitoring module to reliably detect failures in networks with high propagation losses due to either extended reach and/or high client count. In addition, the MON RX takes around ~ 524 ns to detect the falling edge of $\lambda_M$, indicating the absence of $\lambda_M$ and hence working path failure [14].

In this work, we critically study the four power-saving capable survivable HPCAN architectures by evaluating their performance metrics, including connection availability, failure-impact-factor, yearly network energy consumption, and incremental network cost. We consider these architectures to serve three different population densities, namely dense urban, urban, and rural areas, and under three different deployment scenarios, namely brownfield, duct reuse, and greenfield. Specifically, we dimension the survivable HPCAN architectures to serve Berlin, Helfenberg, and Miesbach, representing dense urban, urban, and rural densities respectively. The aim is to connect any building and MBS of an area to the MCO whilst minimizing the required equipment and infrastructure. Through this study, we provide guidance on the best survivable HPCAN architecture to serve each considered scenario.

The rest of the paper is organized as follows. In Section II, the motivation behind the design of survivable HPCAN architectures that can accommodate sleep/doze mode transceivers, is discussed. In Section III, detailed descriptions of the four survivable HPCAN architectures are provided. In Section IV, details of network planning for the three different German cities/towns, each representing a different population density, are presented. In Section V, details of the evaluation of connection availability, Failure Impact Factor (FIF), yearly

network energy consumption and total incremental network cost for each of the four survivable HPCAN architectures and for the unprotected architecture, are presented. The end of the section is devoted to the overall comparison of the four survivable HPCAN architectures serving three area densities under three different deployment scenarios, as well as some guidelines for the selection of the best survivable architecture to be deployed in each of the considered case. Lastly, a brief summary of the main findings of this paper is provided in Section VI.

## II. MOTIVATION

As discussed in Section I, Loss-of-Signal (LOS) is commonly used in conventional networks to detect the occurrence of an equipment/fiber failure and to trigger protection switching of the affected traffic onto the backup path. According to ITU-T G.775 (Loss of Signal, Alarm Indication Signal and Remote Defect Indication defect detection and clearance criteria for plesiochronous digital hierarchy signals), an LOS alarm will be activated at the headend when an incoming signal has no transitions over a period of $175\pm75$ contiguous pulse intervals [15]. For a 10 Gbps line-rate considered in this work, this period of $175\pm75$ contiguous pulse intervals is equivalent to $175\pm75$ ns. Further, as stated in [15], a signal with no transitions is defined as one where the signal level is lower than or equal to 30 dB below nominal, $P_{-30dBnom}$. In a conventional network, an ONU with no uplink data to transmit during idle periods will still send a CW signal with power level $> P_{-30dBnom}$ to ensure LOS alarm is not erroneously activated at the headend. In this case, a signal of power level $< P_{-30dBnom}$ will be detected at the MCO only if a link failure has occurred.

However, in an energy-efficient HPCAN, ONUs and MBSs should be able to transition from *active* to *doze* state (transmitter powered down) or to *sleep* state (both transmitter and receiver powered down) when no uplink data is to be transmitted. When in doze or sleep state, the output transmit power is zero. In cases where all the transmitters are powered down to improve energy-efficiency, e.g. after hours in a shopping center or outside event times in a stadium, one cannot use the absence of upstream signals on the feeder fiber to reliably detect failures as this would cause erroneous triggering of LOS alarm. Our reflective survivable architectures do not need upstream transmissions to trigger LOS alarm, and can therefore be implemented in these instances. As such, failures can be continuously monitored even after hours or outside event times.

In situations where network load is highly variable throughout the day, the idle periods between successive transmissions during low network loads can also erroneously trigger LOS alarm if one uses the absence of upstream transmissions to indicate failures. To explain, let us consider a 10 Gbps passive optical network that is connected to 32 ONUs as an illustrative example. Here, static Time Division Multiple Access (static TDMA) is implemented in the upstream direction to ensure each ONU is provided with a fixed transmission duration once every polling cycle. Fig. 2(a) shows a typical normalized upstream load of the access network vs time of day. A normalized network load of 1 represents 10 Gb/s upstream traffic aggregated from 32 ONUs.

From Fig. 2(a), there are two peak periods, one around noon time and the other around 2000 hour. As discussed, each ONU transmits once per polling cycle, $T_{poll}$. The exact value of $T_{poll}$ to be implemented depends on the maximum tolerable end-to-end delay that is specified as a quality-of-service constraint. Here, we arbitrarily choose $T_{poll}$ to be 2 ms. Fig. 2(c) shows the timing diagram of the upstream transmissions (from all ONUs) that arrive at central office during peak and off peak periods. During peak periods and assuming all ONUs have equal network loads, the transmission time of each ONU, i.e. $T_{ON1} = T_{ON2} = \dots = T_{ON32} = T_{ON}$ is long and the non-transmission time between each successive upstream transmission on the feeder fiber, $T_{OFF1} = T_{OFF2} = \dots = T_{OFF32} = T_{OFF}$ is short. Likewise, during off-peak periods, $T_{ON}$ is short and $T_{OFF}$ is long. In addition to the aggregate network load from all ONUs, the actual duration of $T_{ON}$ and $T_{OFF}$ is also dependent on the polling cycle and the number of supported ONUs.

Fig. 2(b) plots $T_{OFF}$ vs time of day. As discussed, a LOS alarm will be activated at the MCO if optical power is $< P_{-30dBnom}$ over a period of $175\pm75$ ns [15]. If we choose the longest allowable period to be 250 ns, i.e. green line in Fig. 2(b), then one can observed that $T_{OFF} > 250$ ns for most of the day. Typically, transceivers output a CW light with power level $> P_{-30dBnom}$ to prevent triggering the LOS alarm when no upstream transmission is required. However, in the case of energy-efficient networks, transceivers are expected to transition to doze or sleep mode with zero output transmitting power during $T_{OFF}$. If LOS of upstream transmissions is used to detect equipment/fiber failure, the absence of upstream signals during $T_{OFF}$ with duration of more than 250 ns will erroneously trigger the LOS alarm. In our illustrative example shown in Fig. 2(a) and Fig. 2(b), it can be observed that LOS alarm will be erroneously triggered for most of the day.
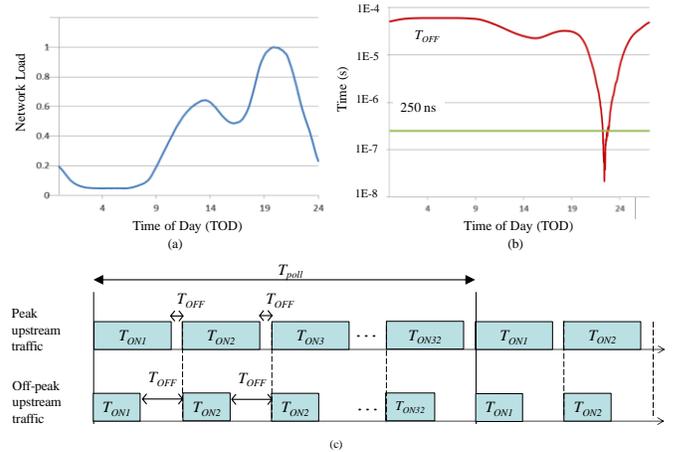


Fig. 2. (a) Network load vs. time of day (TOD), (b) Non-transmission time $T_{OFF}$ between each successive upstream transmission on the feeder fiber, (c) Timing diagram of upstream transmissions on the feeder fiber during peak and off-peak periods.

To alleviate this problem, if $T_{OFF}$ is deterministic, the central office can account for when $T_{OFF}$ is $< P_{-30dBnom}$. For example, in [16]-[17], a timer is activated in the absence of upstream transmissions. Upon expiry of the timer, the LOS alarm is raised to initiate protection switching. The duration of this timer accounts for all Time of Day (TOD) activity to ensure that an alarm is raised only when a genuine failure occurs. Nonetheless, this solution is inflexible to network and traffic

changes as the $T_{OFF}$ of each ONU at each time instance of day needs to be known beforehand. The solution is also unsuitable when dynamic bandwidth allocation schemes that are better suited to dynamic traffic, are implemented instead of static TDMA. With dynamic DBA schemes, $T_{OFF}$ is dynamically varied to minimize delay whilst maximizing throughput and utilization.

The survivable HPCAN architectures proposed in this work, overcome these limitations to provide a more flexible solution in detecting network failures and activating protection switching. Our proposed architectures use monitoring modules with very fast fault detection times of ~524 ns [13]. Similar to the work reported in [18], the architectures rely on the transmission and reflection of a monitoring signal to detect failures. However, unlike [18] which supports only a passive splitter based ODN, the HPCAN architectures proposed in this work supports wavelength aggregation/de-aggregation in the ODN. With the monitoring module, a fast fault detection time is crucial as the overall network restoration time is dependent not only on the network recovery time, i.e., time it takes for backup equipment to establish connection with affected ONUs/MBSs so that they can return to operation state, but also the time it takes to detect network failures. Using our proposed schemes, failures can be identified earlier at the MCO as compared to monitoring upstream transmissions from ONUs. Hence, the outage duration and, consequently, the penalty on operators is reduced.

### III. SURVIVABLE ARCHITECTURES

Descriptions of the four survivable HPCAN architectures are presented in this section. All of the proposed architectures facilitate protection to the MBS due to higher availability requirements as compared with residential users. However, these architectures can be easily extended to any types of users. The architectures are termed: (a) reflective disjoint fiber protection (R-DFP) HPCAN; (b) reflective ring feeder fiber protection (R-RFFP) HPCAN; (c) reflective Disjoint MBS DF Protection (R-DMBSP) HPCAN; and (d) reflective microwave MBS protection (R-μWP) HPCAN. For all proposed architectures, a two stage network is considered to better reflect deployments in practical scenarios. Wavelength de/multiplexing is performed in RN1 whereas power splitting is performed in RN2. In addition, active component(s) added to the network to achieve survivability are confined only to the MCO and/or MBS. The ODN maintains its passive nature, and allows RN2 to reuse the power-splitting ODN of legacy TDM-PONs if required. Further, the fiber link between the MCO and RN1 is denoted as feeder fiber (FF), and that between RN1 and RN2 is denoted as distribution fiber (DF).

### A. Reflective Disjoint Fiber Protection (R-DFP)

The schematic diagram of the reflective disjoint fiber protection (R-DFP) HPCAN is shown in Fig. 3. Here, the standard definition of disjointness is considered whereby disjoint fibers are located in different geographically separated ducts. The MCO includes one or several PON Optical Line Terminals (OLTs) and some other components such as optical switches for protection. In R-DFP, protection is achieved by

using disjoint FF and DF to each MBS. Compared to an unprotected HPCAN, additional equipment is required to
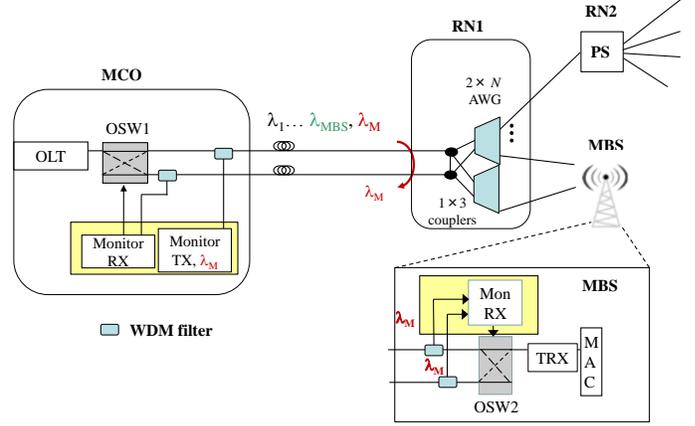


Fig. 3 Reflective Disjoint Fiber Protection (R-DFP) and Reflective Ring Feeder Fiber Protection (R-RFFP) architectures.
\
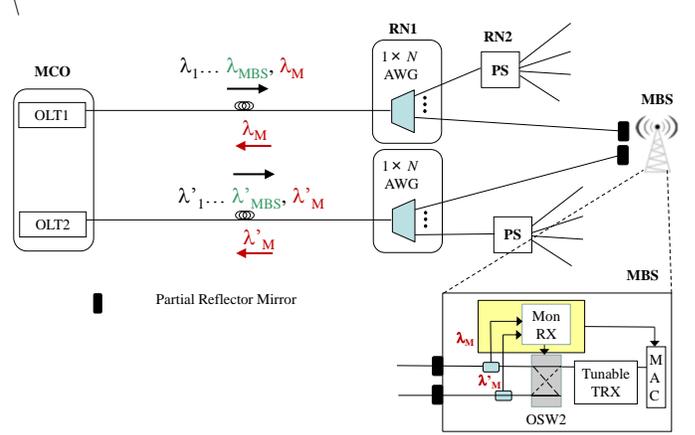


Fig. 4. Reflective Disjoint MBS DF Protection (R-DMBSP) architecture.
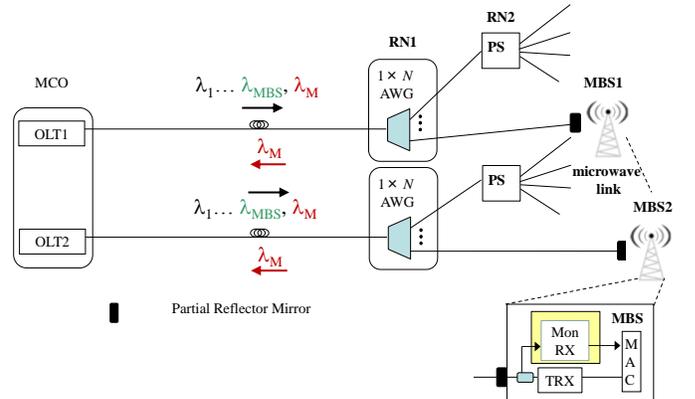


Fig. 5 Reflective Microwave MBS Protection (R-μWP) architecture.

facilitate protection. These comprise an optical switch (OSW1), two WDM filters, and one monitoring module at each OLT, two 1×3 couplers and two 2×N AWGs at RN1, and two 2 WDM filters, one optical switch (OSW2), and one MON RX, at each MBS. Under normal working conditions, $\lambda_M$ is launched into the ODN and a fraction of the optical power of $\lambda_M$ is reflected at the AWG. The reflected $\lambda_M$ is then detected back at the monitoring module at the OLT. Note that

$\lambda_M$ is spaced an integer multiple of the AWG's free spectral range away from the MBS's downstream and upstream wavelength channels. As such, $\lambda_M$ can also be detected at and reflected from the MBS. In the event of a working path failure, $\lambda_M$ is absent at the OLT. This then triggers the OSW1 into CROSS state, and the reassignment of the downstream and monitoring wavelengths. Also, the absence of $\lambda_M$ at the MBS triggers OSW2 into CROSS state and traffic is sent through the protection DF.

### B. Reflective Ring Feeder Fiber Protection (R-RFFP)

The R-RFFP architecture is similar to the R-DFP architecture but with longer feeder fiber link lengths (but shorter ducts due to the duct sharing [9]). In R-RFFP, MBSs are protected through a ring which interconnects all RN1s. In this architecture, each RN1 is connected to two feeder fiber paths that lead to the MCO. The traffic in one feeder fiber propagates in the clockwise direction and the other in the anti-clockwise direction. The shorter feeder fiber path is designated as the working path, i.e. FF, and the longer feeder fiber path is designated as the protection path, i.e. FF'. As in R-DFP architecture, FF and FF' are link disjoint between the MCO and RN1. Likewise, DF and DF' are link disjoint between the RN1 and MBS. As such, R-RFFP requires the same additional components as those discussed in Section III.A.

### C. Reflective Disjoint MBS DF Protection (R-DMBSP)

The R-DMBSP HPCAN architecture is shown in Fig. 4. The DF from each MBS is connected to the closest disjoint RN1 to provide protection to the MBS. As compared to the previous two survivable HPCAN architectures, this solution requires an addition of two partial reflectors at the input to each MBS. Under normal working condition, $\lambda_M$ will be reflected by the partial reflector and detected back at OLT1. In the event of a working path failure, the reflected $\lambda_M$ at OLT1 will be absent thereby triggering the MCO to send downlink data and the monitoring signal towards the MBS using new preassigned wavelengths from OLT2. Meanwhile, the absence of $\lambda_M$ at the MBS will trigger OSW2 into CROSS state, and the MBS will send uplink data on a new pre-assigned wavelength.

### D. Reflective Microwave MBS Protection (R-µWP)

Figure 5 illustrates the survivable R-µWP HPCAN architecture where full network protection is achieved by implementing a microwave link between two disjoint MBSs. In this scheme, it is important that both MBSs are disjointly connected to the MCO and a clear line of sight exists between the two. Under normal working condition, a partial reflector mirror is implemented at the input of each MBS to partially reflect $\lambda_M$ back to the MCO and forward the remaining $\lambda_M$ towards the WDM filter. In the event of a failure on the working path, e.g. that of MBS1, the reflected $\lambda_M$ will be absent at both OLT1 and MBS1. Consequently, the MCO will send downlink data using OLT2, whilst MBS1 will send uplink data to MBS2 via the microwave link. As compared to the unprotected architecture, the R-µWP HPCAN architecture requires the addition of a monitoring module at the OLT, and a combination of a partial reflector, WDM coupler, and RX monitor at each MBS.

## IV. HYBRID CONVERGED ACCESS NETWORK DIMENSIONING

### A. Network Dimensioning

The four survivable HPCAN architectures are compared against an unprotected HPCAN using illustrative examples of three different population densities, namely covering dense urban, urban, and rural areas, and three different deployment scenarios, namely brownfield, duct reuse, and greenfield. Table I summarizes the characteristics of the three considered cities/towns, namely Berlin, Helfenberg, and Miesbach, representing dense urban, urban, and rural densities, respectively. The survivable HPCAN architectures were firstly dimensioned with the aim of (a) connecting all buildings and MBSs of an area to an MCO, and (b) minimizing the equipment and infrastructure required for doing so. For that purpose, the methodology introduced in [9], [19] were applied as follows:

- First the area, i.e. Berlin, Helfenberg, and Miesbach, is selected from Open Street Map (www.openstreetmap.org). The data of the selected area is downloaded, filtered, and parsed as shown in Fig. 6 for the Miesbach rural area.

- The MBS locations in each considered area are then distributed as a grid given an inter-MBS distance. This distribution is related to the required coverage and customer density which is in turn dependent on the type of area, i.e. dense urban, urban or rural. Each type of area has a different population density and hence, requires different MBS density (higher in denser areas). In our evaluation, the MBS density corresponding to dense urban, urban or rural areas was obtained from mobile operators that are participating in the COMBO project [20]. Given the MBS density and the size of the area, the placement is performed according to a grid distribution.



Fig.6 Parsed Rural Area (Miesbach) of 45 km$^2$ with 3103 buildings.
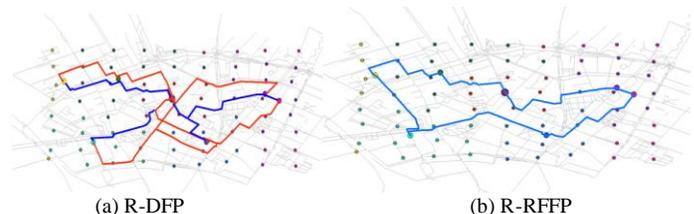


(a) R-DFP  (b) R-RFFP

Fig. 7 FF layout comparison. (a) R-DFP where working (protection) FF is in blue (red), and (b) R-RFFP where traffic on working FF traverse the shortest path from RN1 to MCO, and traffic on protection FF traverse the longer path in the opposite direction to the MCO.

(a)



(b)



(c)
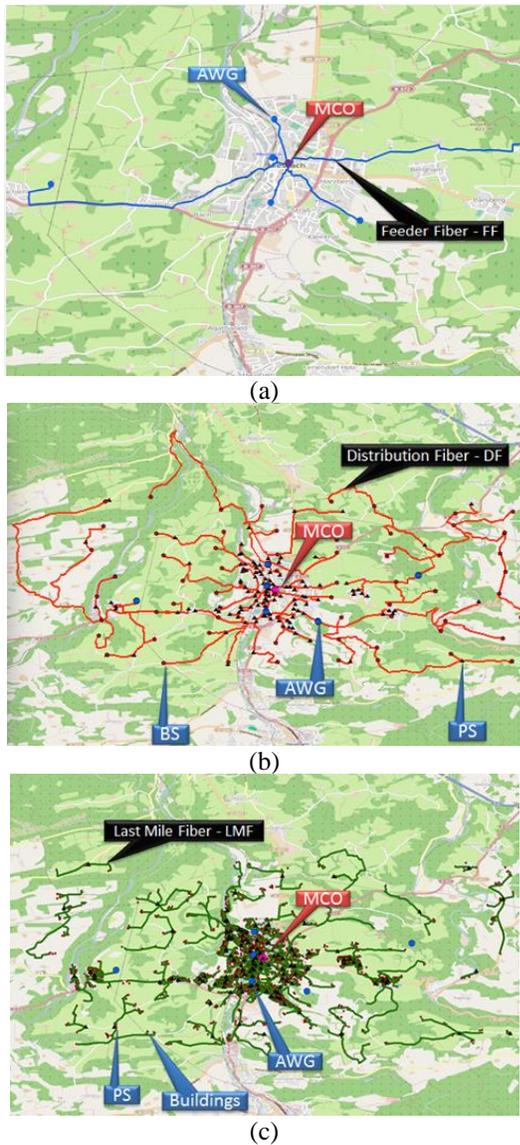
Fig. 8 Fiber layout showing (a) FF, (b) DF, and (c) LMF in Meisbach (rural area).
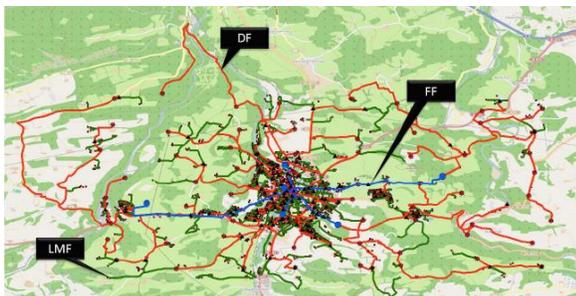


Fig. 9    Total fiber layout (with FF, DF and LMF segments in blue, red and green respectively) in Miesbach (rural area).

- Clustering is then performed to associate buildings to the power splitters at RN2, and to associate RN2 and MBSs to the AWGs at RN1. Cluster size is limited by the splitting ratio and port usage is defined by the operator.

The location of the RN is assumed to be the closest intersection point of the centroid of each cluster.

- Once the locations of all RNs are known, the fiber layout is computed according to the needs of each protection scheme. For example, the FF layout of R-DFP (Section III.A) is different from the FF layout of R-RFFP (Section III.B), as shown in Fig. 7. R-DFP is based on a modification of the shortest path to encourage duct sharing, whereas R-DFFP is computed using the Traveling Salesman Problem (TSP) [21]. In Fig. 7(a). the R-DFP architecture shows the working FF in blue and the shortest disjoint FF, i.e. the protection FF, in red. On the other hand, Fig. 7(b) shows the ring topology of the R-RFFP whereby all RN1 of the primary FF take the shortest path to the MCO with the protection FF taking the longer path in the opposite direction.

- Based on the above methodology, the total fiber and duct required for each segment is calculated, along with the size of the cable needed for each street. Figures 8(a), (b) and (c) show for fiber layout of the FF, DF and Last Mile Fiber (LMF) respectively, for Miesbach (rural area) with Fig. 9 showing the total fiber layout.

### B. Infrastucture Used for Evaluation

We use the unprotected HPCAN architecture as a benchmark to compare the proposed survivable HPCAN architectures under three different area densities and under three deployment scenarios.  Table I summarizes the characteristics of the three considered cities/towns. It is important to note that in the brownfield scenario, we consider fiber costs of already installed dark fibers whereas in the duct reuse scenario, we consider fiber costs that include blowing fiber into already installed ducts.  In the greenfield scenario, we consider fiber costs that includes trenching, laying, and blowing of fiber into new ducts.  The normalized cost of fiber/km in the brownfield and duct reuse scenarios is 4 CU/km and 300 CU/km, respectively [22], where 1 CU represents the cost of a GPON ONU cost. For the greenfield scenario, the normalized cost of CU/km is dependent on the deployment area: namely 1000 CU in dense urban area, 700 CU in urban area, and 400 CU in rural area, respectively [22].  Additionally, in this study, we consider 40 wavelength channel athermal AWGs and 1:32 power splitters. The port utilization is set to 80%, so that the remaining 20% of the ports are left for protection or future use.

TABLE I
CHARACTERISTICS OF THREE CONSIDERED AREA DENSITIES

|  | Dense Urban | Urban | Rural |
|---|---|---|---|
| Location | Berlin | Helfenberg | Miesbach |
| Area [km$^2$] | 3 | 12 | 45 |
| No. of Buildings | 2863 | 2462 | 3103 |
| Buildings/km$^2$ | 954 | 205 | 69 |
| Inter MBS distance [m] | 200 | 400 | 800 |
| MBS/km$^2$ | 24 | 6 | 2 |
| Number of MBS | 72 | 70 | 64 |

TABLE II
INSERTION LOSS/ATTENUATION OF COMPONENTS/FIBER

| Component/fiber | Loss |
|---|---|
| AWG 1:40 | 6.5 |
| AWG 2:40 | 6.5 |
| 1:3 coupler | 9.54 |
| WDM filter | 2 |
| Partial reflector | 3 |
| Feeder fiber/km | 0.25 |
| Distribution fiber/km | 0.25 |

*C. Power budget calculations for reliable monitoring*

In order to reliably detect component/fiber failures using monitoring modules located at the MCO and MBS, the minimum tolerable input optical power level of $\lambda_M$ is limited by the receiver sensitivity of MON RX (~-51 dBm) [14]. In turn, this sensitivity limit forms an upper bound on the allowable transmission distance that can be traversed by $\lambda_M$ and therefore the network reach that can be deployed. As such, a study on (a) the round-trip propagation loss incurred by $\lambda_M$ at the MCO, and (b) single-trip propagation loss incurred by $\lambda_M$ at the MBS, is warranted.

For the survivable R-DFP and R-RFFP HPCAN architectures, $\lambda_M$ is reflected at RN1, incurring a round-trip propagation loss that is given by:

$$RT_{R-DFP,R-RFFP} = 2(Loss_{1:3Coupler} + Loss_{WDMFilter}) + Loss_{FF} + Loss_{FF'} \quad (1)$$

In (1), $Loss_{FF}$ and $Loss_{FF'}$ denote the propagation loss through the working and protection FF, respectively. At the same time, $\lambda_M$ must also be reliably detected at each MBS. The single-trip propagation loss incurred by $\lambda_M$ can be expressed as:

$$ST_{R-DFP,R-RFFP} = 2Loss_{WDMFilter} + Loss_{1:3Coupler} + Loss_{AWG} + Loss_{FF} + Loss_{DF} \quad (2)$$

where $Loss_{DF}$ and $Loss_{pr}$ represent the propagation loss through the DF and the insertion loss of the partial reflector, respectively. Table II lists the typical insertion loss and attenuation values of components and fiber used in our evaluation.

Based on these values, using (1) and (2), and considering +6 dBm launch power, 3dB for aging and repair, -51 dBm receiver sensitivity [14], a 3 dB margin, and 0.25 dB/km fiber attenuation, the maximum allowable transmission distances for R-DFP and R-RFFP are:

$$FF + FF' = \frac{+6 - 2(Loss_{1:3Coupler} + Loss_{WDMFilter}) - 3 - (-51) - 3}{0.25}$$

$$= 112 \text{ km}$$

$$FF + DF = \frac{+6 - (2Loss_{WDMFilter} + Loss_{1:3Coupler} + Loss_{AWG}) - 3 - (-51) - 3}{0.25}$$

$$= 124 \text{ km}$$

For the survivable R-DMBSP and R-μWP HPCAN architectures, $\lambda_M$ is reflected at the partial reflector located at the input of the MBS. The roundtrip propagation loss incurred by $\lambda_M$ can therefore be expressed as:

$$RT_{R-DMBSP,R-\mu WP} = 2(Loss_{AWG} + Loss_{WDMFilter} + Loss_{FF} + Loss_{DF}) + Loss_{pr} \quad (3)$$

At the same time, $\lambda_M$ must also be reliably detected the MBS. However, since the round-trip propagation loss is almost twice as high as that of the single trip, only the power budget constraint arising from the round-trip propagation loss incurred by $\lambda_M$ will limit the maximum allowable transmission distance of R-DMBSP and R-μWP. From (3), the maximum allowable transmission distance is therefore given by:

$$FF + DF = \frac{+6 - 2(Loss_{AWG} + Loss_{WDMFilter}) - Loss_{pr} - 3 - (-51) - 3}{2 \times 0.25}$$

$$= 62 \text{ km}$$

As can be observed from the calculations above, the network span in the R-DFP and R-RFFP HPCAN architectures is determined by the total length of FF and FF' AND by the total length of FF and DF, whilst that of the R-DMBSP and R-μWP HPCAN architectures is determined only by the total length of FF and DF. From the evaluation of the maximum allowable distances above, the use of highly sensitivity monitoring modules facilitate the deployment of network spans that are beyond legacy TDM-PON distances.

V. ANALYSIS OF PROTECTION ARCHITECTURE

*A. Connection Availability*

In this sub-section, the connection availability between an MBS and the MCO is computed and compared across all architectures. Connection availability is defined as the probability of a connection being operational at any point of time. Figures 10 (a)-(c) depict the reliability block diagrams used for computing the connection availability between an MBS and the MCO for the four survivable HPCAN architectures, respectively. The diagrams provide a graphical representation of the relationship between system components from a reliability point of view. Based on the diagrams in Figs. 10(a)-(c), the availability of a connection, $A$, between an MBS and MCO is expressed in (4)-(6) below.

$$A_{R-DFP},A_{R-RFFP} = A_{OLT}A_{OSW1}A_A A_B A_{OSW2}A_{PON-NT} \quad (4)$$

where $A_A = 1 - (1 - A_{WDMFilter}A_{FF}A_{1:3})(1 - A_{WDMFilter}A_{FF'}A_{1:3})$

and $A_B = 1 - (1 - A_{WDMFilter}A_{AWG}A_{DF})(1 - A_{WDMFilter}A_{AWG}A_{DF'})$

$$A_{R-DMBSP} = A_A A_{OSW2}A_{PON-NT} \quad (5)$$

where $A_A = 1 - (1 - A_{OLT}A_{OSW1}A_{WDMFilter}^2 A_{FF}A_{AWG}A_{DF}A_{PR})$
$\times (1 - A_{OLT}A_{OSW1}A_{WDMFilter}^2 A_{FF'}A_{AWG}A_{DF'}A_{PR})$

$$A_{R-\mu WP} = 1 - \left(1 - A_{OLT} A_{OSW1} A^2_{WDMFilter} A_{FF} A_{AWG} A_{DF} A_{PR} A_{PON-NT}\right)$$
$$\times \left(1 - A_{OLT} A_{OSW1} A^2_{WDMFilter} A_{FF} A_{AWG} A_{DF} A_{PR} A_{PON-NT} A_{\mu WP}\right)$$
$$(6)$$

In (4) to (6), parameter $A_i$ denotes the availability of an unprotected link/component/equipment $i$. In turn $A_i$ and $A_j$ are estimated based on their failure characteristics, in particular the mean lifetime and Mean Time To Repair (MTTR). The mean lifetime is provided by the manufacture based on reliability tests made on the equipment/component where as MTTR is provided by the operator based on the fault management policy, equipment and technicians' location, and experience.

With the availability value of different equipment/components listed in Table III, the network connection availability is computed. The connection availability for all survivable architectures and the unprotected architecture is listed in Table IV and shown graphically in Fig. 11. Results show that all survivable architectures have connection availability of at least four nines (at least 99.99%), which is higher than the unprotected architecture (UA). Results also highlight that although R-DFP and R-RFFP have different fiber lengths, they have comparable connection availability, highlighting the fact that once a fiber is protected, the actual deployed fiber length has minor impact on the connection availability. This however, does not apply to the unprotected architecture which connection availability is strongly dependent on the fiber length. Further, results show that R-DMBSP and R-µWP which OLTs are protected have higher connection availability than the other architectures, thereby eluding to the significance in protecting the OLT. Finally, the R-µWP architecture offers the highest connection availability due to full network protection.

*B. Failure Impact Factor*

The Failure Impact Factor (FIF) for each survivable HPCAN architecture is evaluated to measure the impact of a network failure on its users [9]. The FIF for the unprotected and protected HPCAN architectures are given by (7) to (10) below. Observe that the FIF is calculated by summing the individual FIF of each unprotected equipment/fiber in the connection. In turn, the FIF of an unprotected equipment/fiber
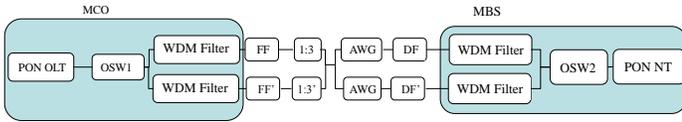
(a) R-DFP and R-RFFP
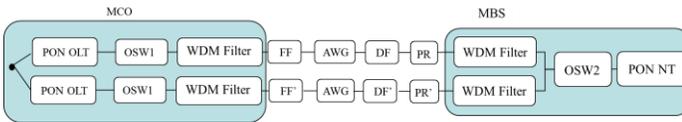
(b) R-DMBSP
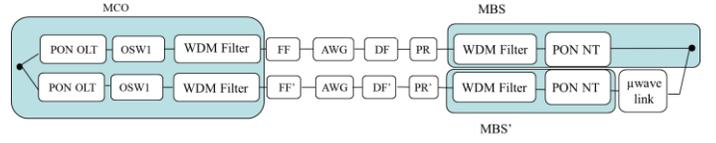
(c) R-µWP

Fig. 10. Reliability Block Diagrams for Survivable HPCAN architectures.
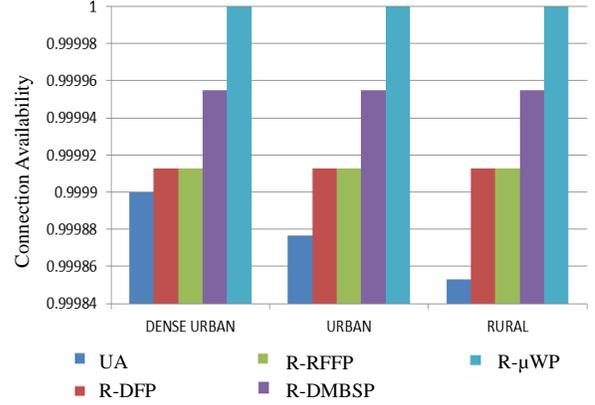
Fig. 11 Connection availability of MBS.

TABLE III
COMPONENT PARAMETERS

| | Availability, $A$ | Cost | Power |
|---|---|---|---|
| OLT | 0.99996381 | 463 | 370 |
| 10 Gbps ONU PON NT | 0.999961 | 3.1 | 5.5 |
| OS | 0.999994 | 2 | 1 |
| PS 1:32 | 0.999999 | 6.6 | 0 |
| PS 2:32 | 0.999999 | 6.8 | 0 |
| AWG 1:40 | 0.999994 | 12.0 | 0 |
| AWG 2:40 | 0.999994 | 14.4 | 0 |
| Filter | 0.999994 | 1.5 | 0 |
| coupler | 0.9999993 | 1 | 0 |
| WDM coupler | 0.9999993 | 1 | 0 |
| TX Mon | 0.9999994 | 1.5 | 1 |
| RX Mon | 0.9999994 | 1.5 | 1 |
| Partial reflector | 0.999999 | 1 | 0 |
| wireless link | 0.999967 | 150 | 18 ON 4 SLEEP |
| Fiber/km | 0.999985725 | 4 (Brownfield) | 0 |
| | | 300 (Duct reuse) | 0 |
| | | 400 (Greenfield – Dense Urban) | 0 |
| | | 700 (Greenfield – Urban) | 0 |
| | | 1000 (Greenfield – Rural) | 0 |

TABLE IV
CONNECTION AVAILABILITY

|  | Dense Urban | Urban | Rural |
|---|---|---|---|
| UA | 0.999899699 | 0.999876776 | 0.999853054 |
| R-DFP | 0.999912811 | 0.999912810 | 0.999912806 |
| R-RFFP | 0.999912810 | 0.999912806 | 0.999912775 |
| R-DMBSP | 0.999954993 | 0.999954987 | 0.999954978 |
| R-µWP | 0.999999978 | 0.999999965 | 0.999999945 |

TABLE V
FAILURE IMPACT FACTOR

|  | Dense Urban | Urban | Rural |
|---|---|---|---|
| UA | 0.16298065 | 0.1812607 | 0.231546 |
| R-DFP | 0.13385265 | 0.1154799 | 0.14443 |
| R-RFFP | 0.13385265 | 0.1154799 | 0.14443 |
| R-DMBSP | 4.6E-05 | 4.6E-05 | 4.6E-05 |
| R-µWP | 0 | 0 | 0 |

is computed by multiplying its unavailability with its Failure Penetration Range (FPR), defined as the number of affected users/connections when this component fails [23]. Using (7) to (10), the FIF of the unprotected and survivable HPCAN architectures are summarized in Table V. Observe that all survivable HPCAN architectures have lower FIF than the unprotected. The R-DMBSP architecture has a significantly lower FIF than R-DFP and R-RFFP due to protection of the OLT at the MCO, again highlighting the importance of protecting the OLT. Further, observe that R-DFP and R-RFFP have identical FIF even though the FF and FF' link lengths are longer in the R-RFFP. This is because fiber is protected in these architectures, and are therefore not included in the calculation of FIF. Eliminating the FIF contribution of fiber, the unprotected components/equipment in R-DFP and R-RFFP are therefore identical as shown in Eqn. (8). Finally, R- µWP has zero FIF due to the fact that it is fully protected and the users are not affected by a single failure in the network.

$$FIF_{UA} = FIF_{OLT} + FIF_{FF} + FIF_{AWG} + FIF_{DF} + FIF_{ONU} \quad (7)$$

$$FIF_{R\text{-}DFP/R\text{-}RFFP} = FIF_{OLT} + FIF_{TRXMON\_OLT} + 2FIF_{WDMCOUPLER\_OLT}$$
$$+ FIF_{OSW1} + FIF_{OSW2} + FIF_{RXMON\_ONU} +$$
$$FIF_{ONU} \quad (8)$$

$$FIF_{R\text{-}DMBSP} = FIF_{OSW2} + FIF_{RXMON\_ONU} + FIF_{ONU} \quad (9)$$

$$FIF_{µWP} = 0 \quad (10)$$

### C. Yearly Network Energy Consumption

It is imperative that the use of fiber/equipment redundancy and microwave links to implement protection in a network does not come at a significant increase in total network cost and network power consumption. Fig. 12 summarizes the total yearly network energy (kWh) consumed by the unprotected and survivable HPCAN architectures, evaluated using the power consumption values outlined in Table III. Note that in evaluating the total yearly network energy, components and equipment in both working and protection paths of each architecture, are taken into account.

From Fig. 12, it can be observed that the proposed protected HPCAN architectures consume more energy than that of the

unprotected HPCAN architecture. Results show that the deployment of survivable HPCAN architectures in rural areas consumes the least energy across all considered architectures due to lower numbers of supported OLTs and MBSs. Overall, the incremental yearly energy consumption over the unprotected architecture is small (8.5% in the worst case for R-µWP in urban area due to the power consumption of the microwave link) in return for a significant increase in connection availability (7 nines for R-µWP in the urban area as compared to 3 nines for UA in the urban area) as discussed in Section V.A. Since we consider all ONUs/MBSs to be active at all times in our calculations shown in Fig. 12, these results represent the worst case (highest possible energy consumption). In reality, in our HPCAN architectures, the ONUs/MBSs will be allowed to sleep or doze to save energy,
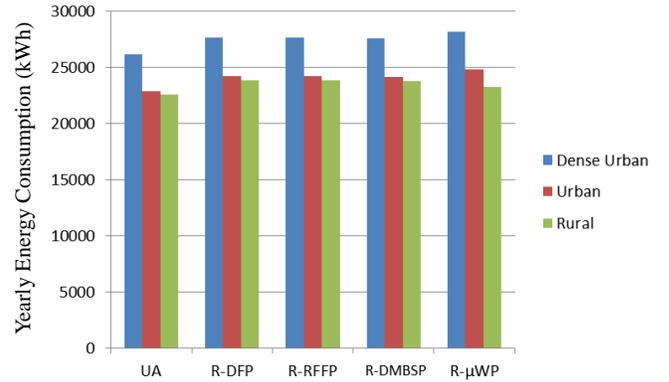


Fig. 12 Yearly network energy consumption (kWh) as function of population densities.

and therefore the incremental energy consumption over the unprotected architecture will be even smaller than that indicated in Fig. 12.

### D. Incremental Network Cost

Network operators are constantly re-evaluating the investments made to provide high bandwidth and resilience in return for revenues from high-value customers. Since the telecom market is currently very competitive, revenues per service are limited. The additional cost incurred from implementing redundancy and monitoring modules in each of the proposed survivable HPCAN architecture is therefore investigated and compared to the unprotected architecture. Figure 13 summarizes the incremental cost (in percentage) incurred for all population densities and deployment scenarios. In our evaluation, the cost of both working and protection paths are considered. The cost unit (CU) of each equipment/component (normalized to a GPON ONU cost) is listed in Table III. As expected, the proposed survivable HPCAN architectures cost higher than the unprotected architecture.

Apart from the R-µWP architecture, rural deployment is characterized by the highest incremental cost across all survivable architectures under all deployment scenarios due to long fiber lengths. Nonetheless, the increase in capital investment to offer protection should be compared with the decrease in penalties caused by service disruption as highlighted in Fig. 11. Considering only the brownfield deployment, the incremental cost of R-µWP is the highest

regardless of the population density. This is because the R-μWP requires the implementation of one microwave link per pair of MBSs for protection. The aggregate cost of all microwave links, each at 150 CU, therefore dominates. The R-RFFP has the second highest incremental cost in the brownfield scenario due to long fiber lengths used in both working and protection paths of this ring architecture.

In the greenfield deployment, out of all architectures considered, the R-RFFP incurs the highest incremental cost due to the fact that the required aggregate fiber length of the working and protection paths is the longest. By contrast, the R-μWP architecture incurs the lowest incremental cost since this architecture does not rely on the use of protection fiber to achieve full protection. The aggregate cost of microwave
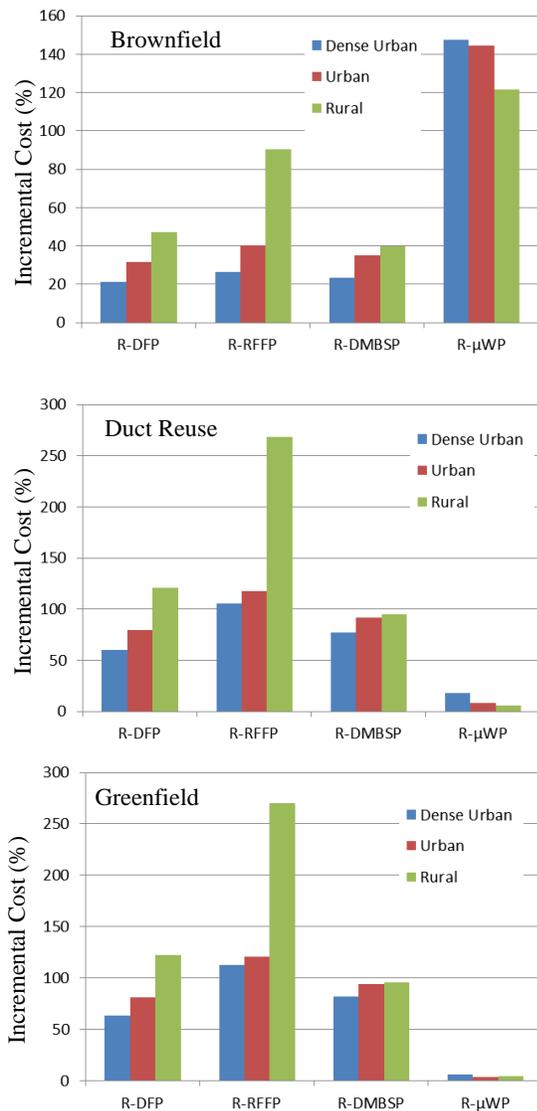


Fig. 13 Total network cost increase with respect the unprotected access architecture

links is not as significant here as that of the fiber which has a cost of 1000 CU/km. The same trends and explanations can be applied to the results computed for the duct reuse case, whereby the cost of fiber/km (includes fiber blowing into existing ducts) is 300 CU/km.

*E. Comparative analysis*

We summarize the comparison between the proposed survivable architectures and the unprotected architecture using net diagrams [23] with the following parameters: (a) cost per MBS (unprotected network cost plus cost of all protection components/equipment including cost of total protection fiber): (b) protection fiber per MBS (in meters), (c) network connection availability, (d) FIF, and (e) yearly network energy per MBS (including unprotected network plus all additional components/equipment for protection). Note that in interpreting a net diagram, the lower the degree, the better the performance. Figures 14 to 16 show the net diagrams of the brownfield, duct reuse, and greenfield deployments, respectively. The proposed degrees and corresponding ranges are represented in the table below each of the net diagrams. Observe that the degrees and chosen ranges for all three tables are identical except for the first column which corresponds to the total network cost parameter. Varying the deployment scenario greatly affects the deployment cost, e.g. fiber cost is 1000 CU/km in rural greenfield vs 4 CU/km rural brownfield. Therefore, to provide a fair comparison of deployment cost between the three area densities under a single deployment scenario, a separate range of cost is necessary.

Figure 14 shows the net diagram of the brownfield deployment, where the R-μWP architecture incurs the highest cost and energy consumption due to expensive and power-consuming microwave links. This is especially significant in the dense urban area due to higher numbers of supported OLTs and MBSs. However, the R-μWP architecture yields the best connection availability and FIF, and uses the least amount of additional protection fiber. In the brownfield deployment, the R-DMBSP HPCAN architecture offers the best compromise for all parameters considered. In both the duct reuse (refer to Fig. 15) and greenfield deployments (refer to Fig. 16), the R-μWP HPCAN architecture offers the best compromise in performance. This architecture incurs an incremental energy consumption of up to 8% as compared to the unprotected HPCAN, and provides high connection availability with zero failure impact factor. It also incurs the lowest total network cost for all area densities considered since the aggregate cost of microwave links is not as significant as that of the fiber.

## VI. CONCLUSION

This paper proposes four survivable architectures to protect against high-impact failures on the working path of future HPCANS. The architectures do not need to rely on loss-of-signal in the upstream direction to trigger protection switching. To compare the four survivable architectures, detailed evaluations of connection availability, failure-impact-factor, yearly network energy consumption, and incremental network cost have been carried out. Results from this study provide guidance for the choice of the best survivable HPCAN architecture to serve each of the three considered area densities under each of the three deployment scenarios. The R-μWP architecture offers the best solution in duct reuse and greenfield deployments. Though incurring an incremental network energy consumption of up to 8% as compared to the unprotected HPCAN, the R-μWP delivers high connection availability with zero failure impact factor at the lowest total

network cost for all area densities considered. For the brownfield scenario, R-DMBSP offers the best solution, providing high connection availability, low FIF, whilst incurring the lowest total network cost and incremental network energy irrespective of area density.
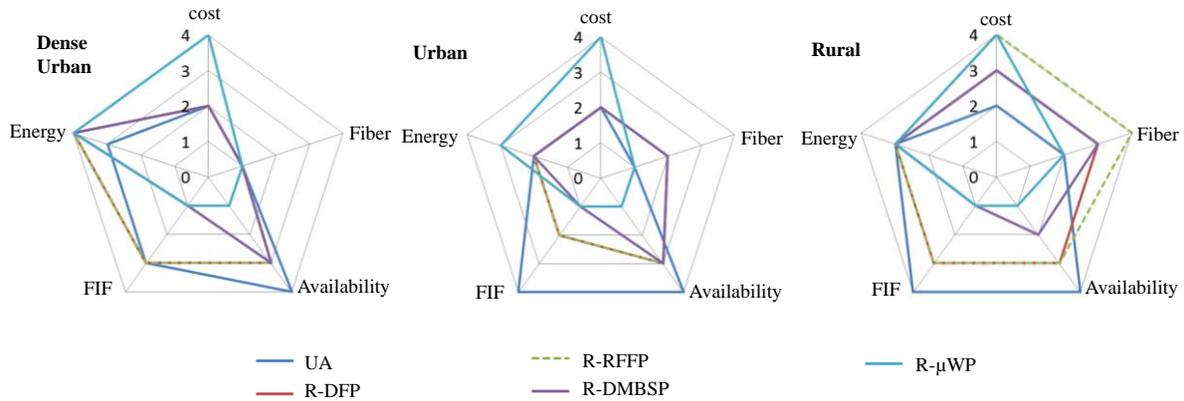


| Degree | Cost per MBS (Cost Unit, CU) | Protection fiber length per MBS (m) | Connection Availability | Failure Impact Factor | Yearly protection energy per MBS (kWh) |
|---|---|---|---|---|---|
| 1 | <40 | <4000 | >. 999999 | <0.06 | <325 |
| 2 | 41-80 | 4001-8000 | > .99999 | 0.061-0.12 | 326k-350 |
| 3 | 81-120 | 8001-12000 | > .9999 | 0.121-0.18 | 351k-375 |
| 4 | >120 | >12001 | > .999 | >0.18 | >375 |

Fig. 14 Net Diagram: Comparison in brownfield deployment
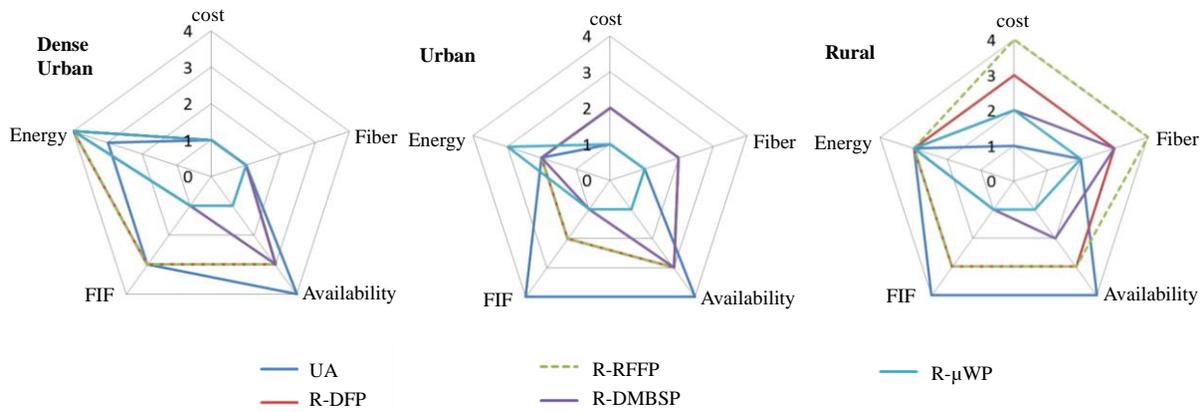


| Degree | Cost per MBS (Cost Unit, CU) | Protection fiber length per MBS (m) | Connection Availability | Failure Impact Factor | Yearly protection energy per MBS (kWh) |
|---|---|---|---|---|---|
| 1 | <1500 | <4000 | >. 999999 | <0.06 | <325 |
| 2 | 1501-3000 | 4001-8000 | > .99999 | 0.061-0.12 | 326k-350 |
| 3 | 3001-4500 | 8001-12000 | > .9999 | 0.121-0.18 | 351k-375 |
| 4 | >4500 | >12001 | > .999 | >0.18 | >375 |

Fig. 15 Net Diagram: Comparison in duct reuse deployment.
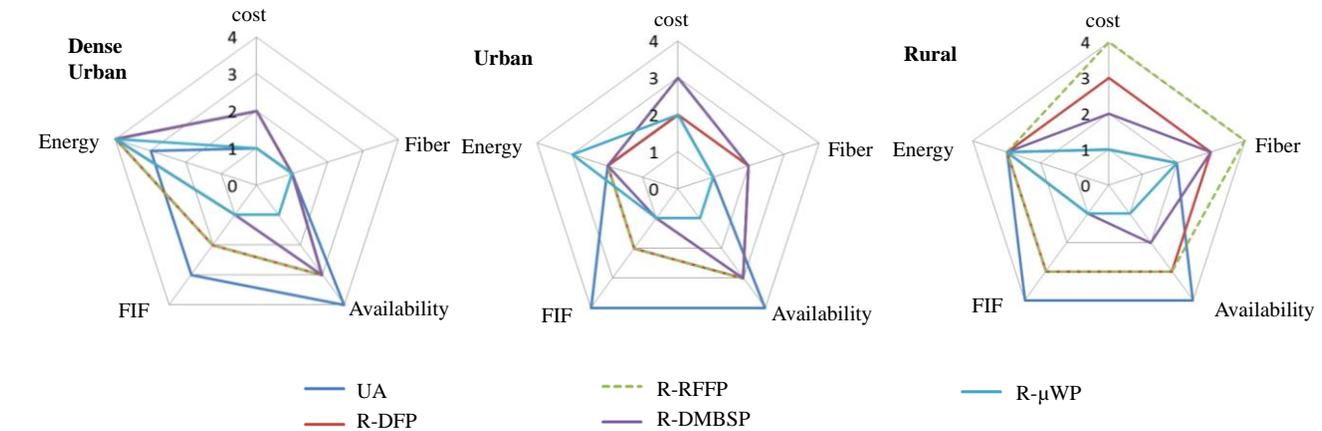
Fig. 16 Net Diagram: Comparison in greenfield deployment.

| Degree | Cost per MBS (Cost Unit, CU) | Protection fiber length per MBS (m) | Connection Availability | Failure Impact Factor | Yearly protection energy per MBS (kWh) |
|---|---|---|---|---|---|
| 1 | <2000 | <4000 | >. 999999 | <0.06 | <325 |
| 2 | 2001-4000 | 4001-8000 | > .99999 | 0.061-0.12 | 326k-350 |
| 3 | 4001-6000 | 8001-12000 | > .9999 | 0.121-0.18 | 351k-375 |
| 4 | >6001 | >12001 | > .999 | >0.18 | >375 |

REFERENCES

[1] E. Wong, "Next-Generation Broadband Access Networks and Technologies," *J. Lightw. Technol*, vol. 30, pp. 597-607, 2012.

[2] H. Nakamura, "NG-PON2 Technology," in *Proc. of IEEE/OSA Opt. Fiber Commun. Conf.*, Anaheim, USA, NTh4F.5, 2013.

[3] C. Mas Machuca and W. Kellerer, "Planning methodology towards next generation optical access networks," *Networks 2014*, Portugal, September 2014.

[4] M. Ruffini, E. Di Pascale, D.B. Payne, "Discus: End-to-end network design for ubiquitous high speed broadband services," in *Proc. of Transparent Optical Networks (ICTON), 2013*, pp. 1–5, 2013.

[5] A. Dixit, B. Lannoo, D. Colle, M. Pickavet, and P. Demeester, "Wavelength swichted hybrid TDMA/WDMA PON: A flexible next generation optical access solution [Invited]," in in *Proc. of Transparent Optical Networks (ICTON), 2014*, Coventry, UK, July 2012.

[6] J. Chen and L. Wosinska, "Analysis of Protection Schemes in PON Compatible with Smooth Migration from TDM-PON to Hybrid WDM/TDM PON", *OSA Journal of Optical Networking*, vol. 6, May, 2007, pp. 514-526.

[7] N. Nadarajah, A. Nirmalathas, and E. Wong, "Self-protected Ethernet passive optical networks using coarse wavelength division multiplexed transmission", *IEE Electronics Letters*, vol. 41, pp. 866-867, July 2005.

[8] M. A. Esmail and H. Fathallah, "Fiber Fault Management and Protection Solution for Ring-and-Spur WDM/TDM Long-Reach PON", *Proc. of IEEE Global Telecommunications Conference*, (2011), Dec. 2011, pp.1-5.

[9] A. Shahid, C. Mas Machuca, L. Wosinska, and J. Chen, "Comparative Analysis of Protection Schemes for Fixed Mobile Converged Access Networks based on Hybrid PON", *2015 Conference of Telecommunication, Media and Internet Techno-Economic Proceedings*, Munich, Germany, 2015.

[10] A. Shahid "Enhanced dimensioning and comparative analysis of different protection schemes for Hybrid PON Converged Access Networks (HPCAN)" *Technical report 201502 TUM*, LKN, 2015.

[11] J. Baliga, R. Ayre, K. Hinton, W.V.Sorin, and R. Tucker, "Energy Consumption in Optical IP Networks," *IEEE/OSA Journal of Lightwave Technology*, vol. 27, pp. 2391-2401, 2009.

[12] E. Wong, M. Mueller, P.I. Dias, C.A. Chan, and M.C. Amann, "Energy-efficiency of optical network units with vertical-cavity surface-emitting lasers," *Optics Express*, vol. 21, pp. 14960-14970, 2013.

[13] E. Wong, C.M. Machuca, and L. Wosinska, "Survivable Architectures for Power-Savings Capable Converged Access Networks," in *Proc. of ICC 2016*, paper ONS1.4, 2016.

[14] E. Wong and K.L. Lee, "Characterization of highly-sensitive and fast-responding monitoring module for extended-reach passive optical networks," *Optics Express*, vol. 28, pp. 9019-9030, 2012.

[15] ITU-T G.775, Loss of Signal (LOS), Alarm Indication Signal (AIS) and Remote Defect Indication (RDI) defect detection and clearance criteria for PDH signals, 1998, ITU.

[16] S. McGettrick et al., "Ultra-fast 1+1 protection in 10 Gb/s symmetric long reach PON," in *Prof. of European Conference and Exhibition on Optical* Communication (*ECOC 2013*), pp. 1–3, 2013.

[17] F. Slyne, N. Kituswan , S. McGettrick, D.B. Payne, and M. Ruffini, "Design and experimental test of 1:1 end-to-end protection for LR-PON using an SDN multi-tier control plane," in *Prof. of European Conference and Exhibition on Optical* Communication (*ECOC 2014*), pp. 1–3, 2014.

[18] E. Wong, "Survivable architectures for time and wavelength division multiplexed passive optical networks", *Opt. Commun.*, vol. 325, 152-159, 2014.

[19] A. Munoz Diaz, and C. Mas Machuca, "Are Converged Access Networks suitable in rural areas?", in *Proc. of IEEE International Conference on Transparent Optical Networks (ICTON)*, Budapest, Hungary, July 2015.

[20] Available [Online]: http://www.ict-combo.eu/

[21] D. S. Johnson and L. A. McGeoch "The Traveling Salesman Problem:A Case Study in Local Optimization", 1997 :Wiley

[22] Available [Online]: http://www.cablinginstall.com/articles/print/volume-22/issue-8/features/installation/a-comparison-of-conventional-fiber-and-blown-cable.html

[23] M. Mahloo, J. Chen, L. Wosinska, A. Dixit, B. Lannoo, D. Colle, and C. Mas Machuca, "Towards Reliable Hybrid WDM/TDM Passive Optical Networks", *IEEE Communication Magazine*, vol. 52(2), pp. S14-S23, February 2014.